Available online at www.sciencedirect.com

SCIENCE DIRECT®

Journal of Catalysis 236 (2005) 190–204

JOURNAL OF CATALYSIS

www.elsevier.com/locate/jcat

A density functional theory study of the hydrogenolysis reaction of CH_3SH to CH_4 on the catalytically active (100) edge of 2H-MoS_2

T. Todorova, R. Prins, Th. Weber [*]

Institute for Chemical and Bioengineering, Swiss Federal Institute of Technology (ETH), Wolfgang-Pauli-Strasse 10, HCI E 128, CH-8093 Zurich, Switzerland

Received 5 July 2005; revised 20 September 2005; accepted 21 September 2005

Abstract

The breaking of the C–S bond is a crucial step in hydrodesulfurization, the removal of the sulfur atom from sulfur-containing molecules in crude oil. Thus the hydrogenolysis reaction of CH_3SH to CH_4 was studied by means of density functional theory on the catalytically active (100) edge of 2H-MoS_2, with and without Co and Ni promoter atoms. Thiol adsorption, C–S bond breaking, and the formation and desorption of CH_4 were investigated with different sulfur and hydrogen surface coverages. CH_3SH first adsorbs molecularly with its S atom in a bridging mode between two surface Mo atoms, followed by S–H bond cleavage with moderate activation energy. The subsequent concerted C–S bond breaking and CH_4 formation occurs through a reaction of the adsorbed CH_3S group with the H atom of a neighbouring SH group at the molybdenum sulfide surface. Sulfur atoms, hydrogen atoms adsorbed on sulfur atoms, and promoter atoms (Co and Ni) at the catalyst surface weaken the bonding of adsorbed CH_3S and lower the energy barrier for CH_4 formation. Although the reactions of thiols on the metal sulfide surface are similar to reactions on metal surfaces, the chemistry is different. The reactions occur between intermediate alkyl and hydrogen fragments bonded to sulfur atoms, not to metal atoms.

Keywords: Density functional theory; Hydrodesulfurization; C–S bond breaking; Hydrogenolysis; Sulfide catalysis; Molybdenum disulfide; CoMoS

1. Introduction

Crude oil contains organosulfur compounds, such as thiophene and dibenzothiophene, and hydrodesulfurization (HDS) is one of the first steps in its processing. In HDS the sulfur-containing molecules react with hydrogen on the surface of metal sulfide catalysts to form hydrocarbons and H_2S [1–5], after which the H_2S is removed by absorption. HDS will become increasingly important as environmental regulations demand increasingly smaller amounts of sulfur in gasoline and gasoil fuels. Two basic HDS reactions have been identified as being responsible for the removal of sulfur from dibenzothiophene, one of the most difficult components to desulfurize: direct desulfurization and hydrogenation followed by sulfur removal. In the direct desulfurization reaction, dibenzothiophene and H_2 react to biphenyl and H_2S. The hydrogenation reaction involves hydrogenation of one of the benzene rings of dibenzothiophene, followed by desulfurization of the resulting hexahydrodibenzothiophene to yield cyclohexylbenzene. A large body of theoretical research has aimed at understanding the mechanisms of C–S bond breaking of thiophene and dibenzothiophene through their interaction with the metal sulfide catalyst surfaces [6–17]. Organometallic chemistry has also contributed to the understanding of C–S bond breaking. Various modes of thiophene coordination to transition metal complexes, representing different types of adsorption on metal sites in heterogeneous HDS catalysts, have been proposed [18–24].

Notwithstanding the intensive research into HDS, the reaction mechanism of the main route of the HDS of dibenzothiophene—direct desulfurization—remains in dispute. Some believe that the mechanism consists of an actual hydrogenolysis reaction, during which C–S bonds are broken and C–H and S–H bonds form simultaneously, so that biphenyl forms directly from dibenzothiophene and hydrogen on the catalyst surface [1–4]. A related mechanism may be the insertion of a metal atom in the C–S bond, as observed in organometallic

---

[*] Corresponding author. Fax: +41 44 632 1162.
E-mail address: thomas.weber@chem.ethz.ch (Th. Weber).

0021-9517/$ – see front matter © 2005 Elsevier Inc. All rights reserved.
doi:10.1016/j.jcat.2005.09.032

complexes of thiophene and benzothiophene [21,22], followed by hydrogenation. Others argue that the mechanism consists of hydrogenation of dibenzothiophene to dihydrodibenzothiophene, followed by elimination to yield biphenyl and H_2S [25]. The much simpler hydrogenolysis reaction of alkanethiols to alkanes also has not been studied in depth; it is complicated by the parallel elimination reaction of the alkanethiols to alkenes. The HDS of alkanethiols over metal sulfide catalysts is already rapid at 500 K [26]. The reaction is much faster over pure metal surfaces [27]. Thus S–H bond breaking, yielding a $C_nH_{2n+1}S$ fragment and an H atom, already occurs at about 150 K on most metals, and the C–S bond breaking of $C_nH_{2n+1}S$ occurs at somewhat higher temperature but still below room temperature [28–34]. This demonstrates that metals are potentially much better HDS catalysts than metal sulfides. Nevertheless, industrially used HDS catalysts are based on the layered transition-metal sulfides of Mo or W, promoted by Co or Ni [1,2], because metals would quickly become metal sulfides during HDS.

Although the experimental interaction of thiols with metal surfaces has been studied in depth, very little has been published about the interaction of alkanethiols with the surface of metal sulfides. The main reason for this is that it is much more difficult to perform surface science studies of metal sulfide surfaces than of clean metal surfaces. Consequently, many fundamental aspects, such as the initial adsorption geometry, the nature of the catalytically active site, and the mechanism of C–S bond breaking on metal sulfide surfaces, remain unclear. Organometallic studies have addressed mechanistic aspects of the desulfurization of thiols. Curtis and coworkers [35,36] showed that the association of aromatic and aliphatic thiols with a $Cp'_2Mo_2Co_2S_3(CO)_4$ cluster occurs by a rearrangement of the cluster and that the coordination of the thiol to the cluster results in a substantial weakening of its C–S bond energy. They suggested that this association is the rate-determining step in the desulfurization reaction and that the subsequent cleavage of the C–S bond occurs rapidly.

We report the first ab initio computation of the reaction pathways for the dissociation of CH_3SH and for the geometry-optimized HS and CH_3S intermediates on the (100) catalytically active surface of 2H-MoS_2. The effect of Co and Ni promoter atoms and the presence of hydrogen on the surface have been considered as well. We chose the simplest alkanethiol, CH_3SH, because only hydrogenolysis to CH_4 can occur for this molecule. Using density functional theory (DFT), we calculated the minimum energy path for the CH_3SH dissociation with the aim of determining the chronological order of the chemical reaction steps, the various energies of the reactions, and the activation barriers. In this way, we provide information about the chemisorption and reaction of thiols on the (100) catalytically active surface of 2H-MoS_2.

2. Computational details

In DFT calculations, we used the $DMol^3$ code [37,38] with a double-numeric polarized basis set and a medium level of integration grid, amounting to approximately 1000 grid points per atom, and performed effective core potential calculations. Each basis function was restricted to within a cutoff radius of 5.5 Å. The local density approximation was used to specify the exchange-correlation local potential [39] and was corrected in the high- and low-density expansions proposed by Perdew and Wang [40,41]. Brillouin zone integration was performed with a set of 2 × 2 × 1 k-points. Direct inversion in an iterative subspace was used to accelerate the self-consistent field convergence, and a thermal smearing of 3 kcal/mol was applied to the orbital occupation. We selected a surface (4 × 1) super cell of the 2H-MoS_2-crystal structure with a vacuum slab of 9 Å and a slab thickness of 12 Å. The (4 × 1) model surface consists of two MoS_2 sheets in the z direction, six planes of atoms in the y direction (three MoS_2 units), and four surface Mo atoms in the x direction (Fig. 1). The (100) MoS_2 surface exhibits two types of edges. Unsaturated molybdenum atoms are exposed on one edge (hereafter referred to as the Mo edge), whereas sulfur atoms are exposed on the other edge (the S edge). The geometry of all of the atoms in the slabs was optimized. Geometry optimization convergence thresholds of 0.01 kcal/mol, 2.5 kcal/(mol Å), and 0.005 Å were used between the optimization cycles for the energy change, maximum force, and maximum displacement, respectively.

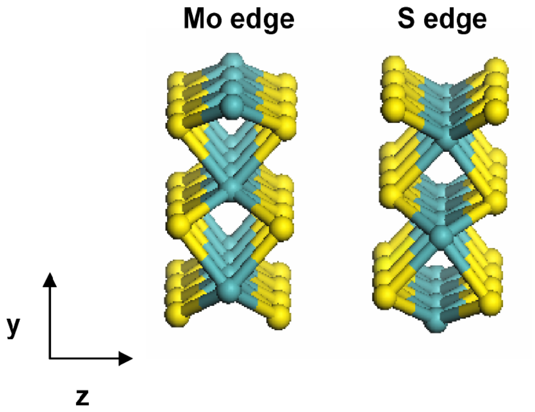

Fig. 1. Schematic representation of the 2H-MoS_2 (100) surface.

The CH_3SH molecule was thermally equilibrated with the surface in the initial state. The activation energy is determined by the highest maximum on the minimum energy path, obtained by the linear/quadratic synchronous transit (LST/QST) method [42]. To calculate the minimum energy path between several reaction steps we used the LST/QST method proposed by Halgren and Lipscomb [43] and implemented in the $DMol^3$ code. The reaction path connects the CH_3SH molecule above the surface with the products, the CH_4 molecule, which is desorbed to the gas phase, and the S atom, which is adsorbed on the catalyst surface. The path was divided into several steps between the reactant and products, and the energies of these steps, as well as the adsorption barriers, were calculated. The success of the calculations through the LST/QST method is based on the close proximity of two immediate stable structures (the endpoints) for the transition state search. The selection of the endpoints for the transition state search was done by an interpolation along the path segments. This is done most accurately in a coordinate system, which naturally follows the adiabatic valley of the potential. Moreover, it reduces the number of intermediate path points to be refined. However, another reaction pathway also may exist. The transition state has been refined by optimizing the transition state following the eigenvector of the Hessian matrix corresponding to the imaginary frequency mode. It has thus been checked that the transition states have only one imaginary frequency.

3. Results

3.1. *Dissociation of CH_3SH*

3.1.1. *Unpromoted Mo edge*

DFT calculations have shown that the Mo edge of MoS_2 crystallites is fully covered with sulfur atoms under conditions that prevail in industrial HDS ($0.01 < H_2S/H_2 < 0.1$) [11,13,15]. Each Mo atom is surrounded by six sulfur atoms, four of which are also linked to two other Mo atoms (as in bulk MoS_2) and two of which are at the surface in bridging positions between the Mo surface atoms. This prediction was confirmed by scanning tunnelling microscopy observations of MoS_2 particles on a gold substrate [44–46]. But a recent DFT calculation on an enlarged Mo edge (with six instead of two or three MoS_2 units, as in previous calculations) predicts that the probability of one sulfur vacancy and five bridged sulfur atoms is at least a few percentage points in the range $0.01 < H_2S/H_2 < 0.1$ [47]. The HDS literature generally assumes that the reacting molecules are adsorbed on vacancies at the catalyst surface; therefore, we studied the reaction of CH_3SH on the Mo edge covered with sulfur atoms in bridging positions between the surface Mo atoms and with at least one sulfur vacancy. Because our model surface contains four surface Mo atoms (Fig. 1), the number of bridging sulfur atoms (N_{br}) was varied from zero to three, and thus the number of sulfur vacancies has varied from four to one.

In a first series of calculations, we started with a CH_3SH molecule located above the bare Mo-terminated edge surface, with the S atom of the CH_3SH molecule 4.5 Å from a surface metal atom (Fig. 2a). To be consistent with our other calculations where sulfur was present on the surface (Figs. 4, 5, and 6), a similar initial state with the S–H bond of the organic molecule parallel to the row of surface metal atoms was selected. The approach of CH_3SH to the surface and activation ($a \rightarrow b \rightarrow c$) were accompanied by energy changes of 12.6 kcal/mol (energy barrier) and −25.1 kcal/mol (reaction energy). The S atom of CH_3SH took a bridge position between two surface metal atoms with a Mo–S distance of 2.5 Å. The H atom from the CH_3SH molecule changed its orientation. In the initial state configuration, the S–H bond was parallel to the row of metal atoms of the surface, whereas in the molecularly adsorbed state, the S–H bond orientation was perpendicular to the metal row. The preference of the relaxed methanethiol for bonding in a bridge site can be considered a compromise between the sulfur atom, which prefers a high coordination to the Mo atoms and the hydrogen atom, which does not adsorb well in the surface plane because of repulsion, in agreement with the findings for other atomic adsorbates at metal surfaces [48]. The C–S bond length increased from 1.8 Å (initial state, a) through 2.0 Å (intermediate state, b) to 2.3 Å (molecularly adsorbed state, c).

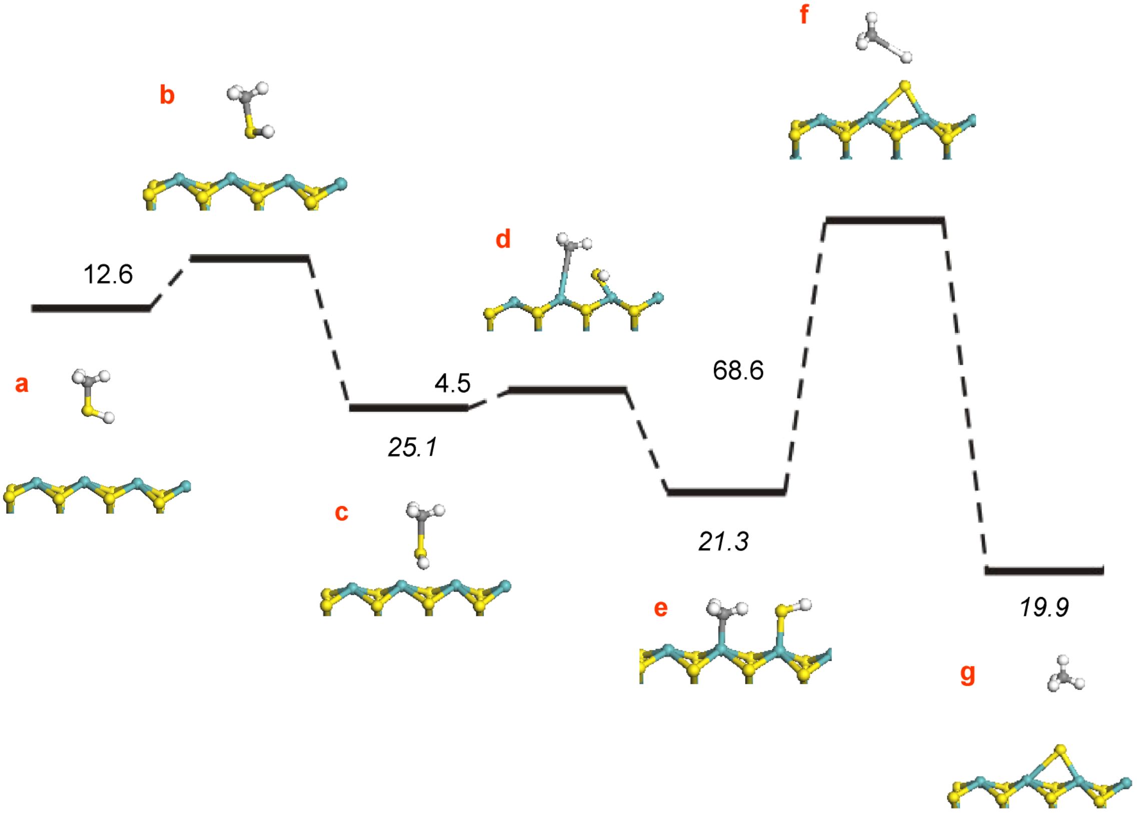

Fig. 2. Reaction path of the reaction of CH_3SH to CH_4 by C–S bond breaking before S–H bond breaking on the bare unpromoted Mo edge of 2H-MoS_2.

C–S bond splitting of the activated CH_3SH molecule and migration of the S–H and CH_3 fragments to two adjacent Mo centres (c → d → e) have an energy barrier of only 4.5 kcal/mol. X-ray photoelectron and high-resolution electron energy-loss spectroscopy have shown that surface $C_nH_{2n+1}S$ intermediates are formed from thiols with an energy barrier < 7 kcal/mol when adsorbed on metallic Mo(110) [49]. The energy of state (e), with adsorbed methyl and SH fragments, was 21.3 kcal/mol lower than that of the state with molecularly adsorbed CH_3SH (c → e). The formation of CH_4 from the adsorbed CH_3 and S–H fragments (e → g) had a high activation barrier (68.6 kcal/mol), due to the strong Mo–C and MoS–H bonds that must be broken. Because the metal atoms on the surface (a) had a coordination number of only four, they attempted to increase the coordination number by adjusting the adsorbed species via the Mo–S and Mo–C interactions. Removing hydrogen from the SH fragment changes the coordination mode of sulfur. The final state, with a CH_4 molecule above the surface and two five-coordinated metal centres on the surface, was energetically the most favourable situation, because in the final reaction step, the energy also decreased, by 19.9 kcal/mol. The remaining sulfur atom clearly prefers a high coordination in a bridging mode between two surface Mo atoms (Fig. 2, g), in agreement with the results of Hammer and Nørskov for transition-metal surfaces [48].

In addition to the reaction path (Fig. 2), in which the C–S bond breaks first, we investigated another hydrogenolysis reaction path in which the S–H bond breaks first (Fig. 3). In the latter case, the H atom and the CH_3S fragment in the intermediate state (e*) were more strongly bound to the surface than the CH_3 and SH fragments in state (e) (Fig. 2). In the intermediate state, the S–C bond length increased to 2.2 Å. Because of the stronger bonding of the intermediates to the surface, the energy barrier to form methane increased to 78.4 kcal/mol (e* → f*). Thus, this step is less likely than step (e → f).

When one sulfur atom is already present on the Mo edge, it tends to take a bridging position between two Mo atoms, the final surface state as shown in Fig. 2 (state g). In calculating the interaction of CH_3SH with this surface, the CH_3SH molecule was initially positioned 4.5 Å above the surface and the C–S bond length was calculated to be 1.8 Å (Fig. 4, h). In the intermediate state (j), the S–H bond is broken and the SCH_3 fragment is adsorbed in a bridging position between two metal atoms, adjacent to the bridging sulfur atom. In this state the C–S bond increased to 2.4 Å. The hydrogen atom went to the preadsorbed adjacent surface sulfur atom, and the S–H bond orientation was perpendicular to the row of surface metal atoms. An energy barrier of 18.8 kcal/mol (h → i) and reaction energy of -38.9 kcal/mol (h → j) was calculated. Another intermediate state for the formation of structure (j) may consist of an adsorbed bridge CH_3S fragment and a Mo–H surface species. We did not consider such intermediate states because Mo–H bonds are rather strong, and the activation energy required for bond breaking is > 18.8 kcal/mol [52]. Once again the coordination of the thiol to the surface was very favourable, as the high exothermicity of the reaction shows. The forma-

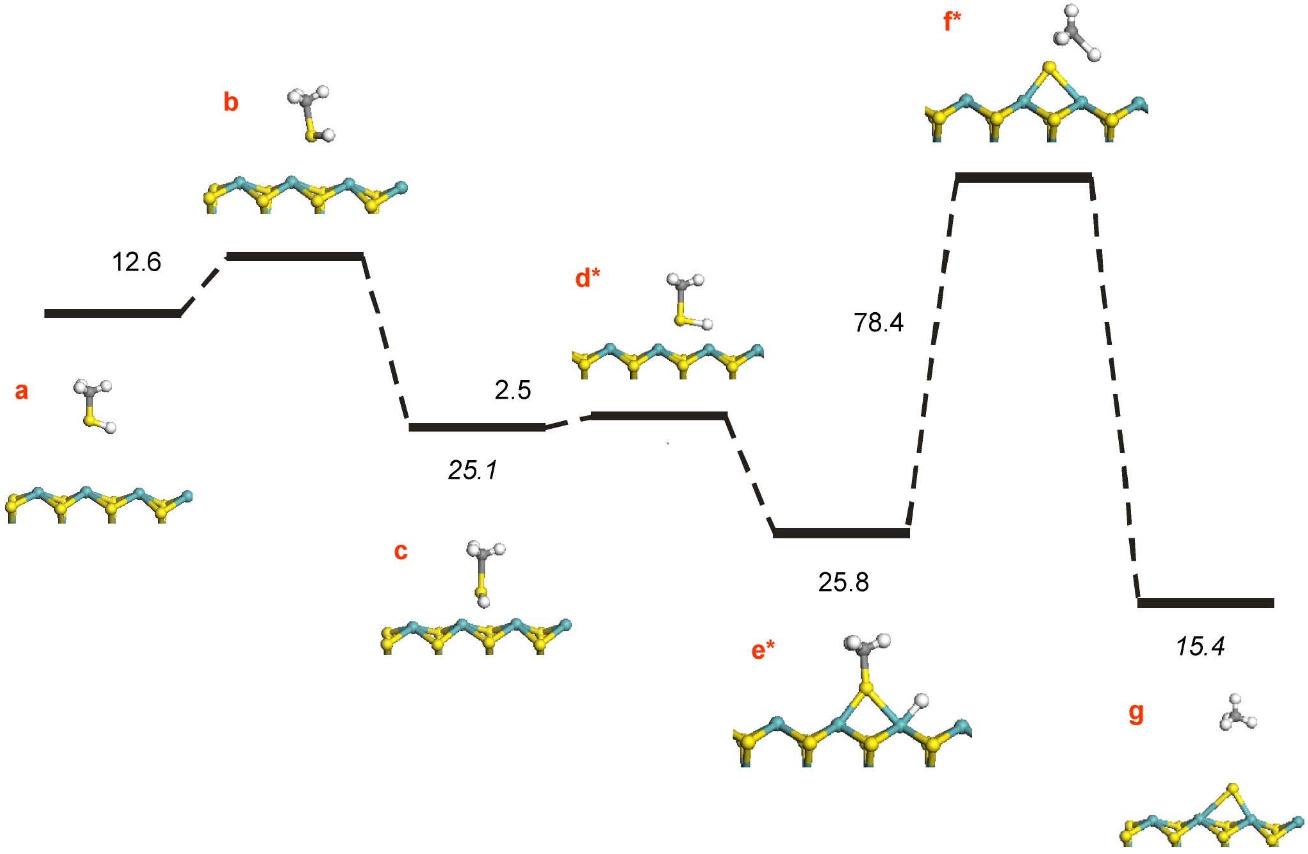

Fig. 3. Reaction path of the reaction of CH_3SH to CH_4 by S–H bond breaking before C–S bond breaking on the bare unpromoted Mo edge of 2H-MoS_2.

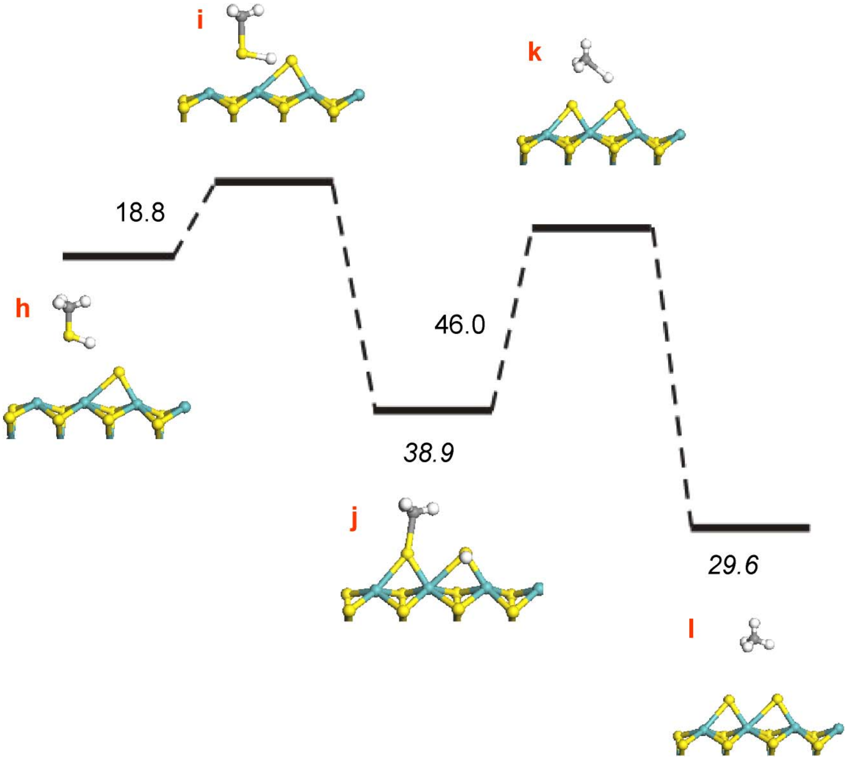

Fig. 4. Reaction path of the reaction of CH_3SH to CH_4 on the unpromoted Mo edge of 2H-MoS_2 with one sulfur atom in bridging position.

tion of CH_4 (j → k) required a rather high activation energy (46.0 kcal/mol) but lower than in the corresponding step in Fig. 2 (68.6 kcal/mol) and Fig. 3 (78.4 kcal/mol). This is due to the presence of a sulfur atom already on the surface, which lowers the metal edge energy by making two of the surface metal centres five-coordinated. The last transition state (k) shows hydrogenation of the CH_3 group with accompanying C–S bond breaking. The final state (l) consists of CH_4 in the gas phase and a Mo-terminated surface with two sulfur atoms in bridging positions.

A third calculation of the hydrogenolysis of CH_3SH on the Mo edge of MoS_2 was performed with two surface vacancies between two bridging S atoms (Fig. 5). Again, in the initial state (m) the CH_3SH molecule was situated 4.5 Å above the surface, with $d(\text{S–C}) = 1.8$ Å. In the intermediate state (o), the CH_3S fragment was adsorbed on the sulfur vacancy and the H atom was adsorbed on a neighbouring sulfur atom. The S–C distance was calculated as $d(\text{S–C}) = 2.4$ Å. The activation (m → n) and dissociation (n → o) of the molecule were accomplished with an energy barrier of 16.6 kcal/mol and reaction energy of -22.9 kcal/mol. The final step was to form CH_4 from the already adsorbed fragments and to remove it from the surface. This step had a barrier of 30.0 kcal/mol (o → p), and the final state (q) was energetically preferred by -55.2 kcal/mol. This activation energy was lower than that of the surface with one S atom (Fig. 4) and demonstrates the positive influence of preadsorbed S atoms.

A fourth calculation of hydrogenolysis of CH_3SH on the Mo edge of MoS_2 was performed with one surface vacancy and three bridging S atoms (Fig. 6). The results were similar to those of the foregoing calculation. In the intermediate state, the CH_3S fragment adsorbed on the sulfur vacancy, and the H atom adsorbed on a neighbouring sulfur atom. The activation energy barrier for adsorption and dissociation was 22.8 kcal/mol, and the reaction energy was -20.1 kcal/mol. The second step, to form CH_4 from the already adsorbed fragments and remove it from the surface, had a barrier of 18.8 kcal/mol and a reaction energy of -61.9 kcal/mol. This second activation energy was even lower than that for the surface with two S atoms (Fig. 5), confirming the positive influence of preadsorbed S atoms. Table 1 gives the results of all calculations with different numbers (N_{br}) of bridging sulfur atoms on the Mo edge.

The influence of surface hydrogen was investigated by letting CH_3SH dissociate on a surface covered with a sulfur atom and a hydrogen atom. In the most stable initial state (Fig. 7, h**), the hydrogen atom is adsorbed on the sulfur atom, forming an SH group. In the intermediate state (j**), the hydrogen atom of methanethiol was preferentially adsorbed on the sulfur atom as well, forming adsorbed H_2S.

The energy barrier for CH_3SH adsorption and dissociation was 22.5 kcal/mol, which is 3.7 kcal/mol higher than the energy barrier in the absence of surface hydrogen (Fig. 4). The hydrogen atom, preadsorbed on the sulfur, creates steric repulsion for adsorption of the second hydrogen atom on the same sulfur. In contrast, formation of CH_4 was easier (j** → k**) compared with the case of the hydrogen-free surface, as shown by the decrease in the desorption barrier of CH_4 to 35.4 kcal/mol from 46.0 kcal/mol for the hydrogen-free surface. The intermediate and final products were more stable on the hydrogenated surface than on the surface without hydrogen atoms. The same calculation was performed starting with a surface covered with

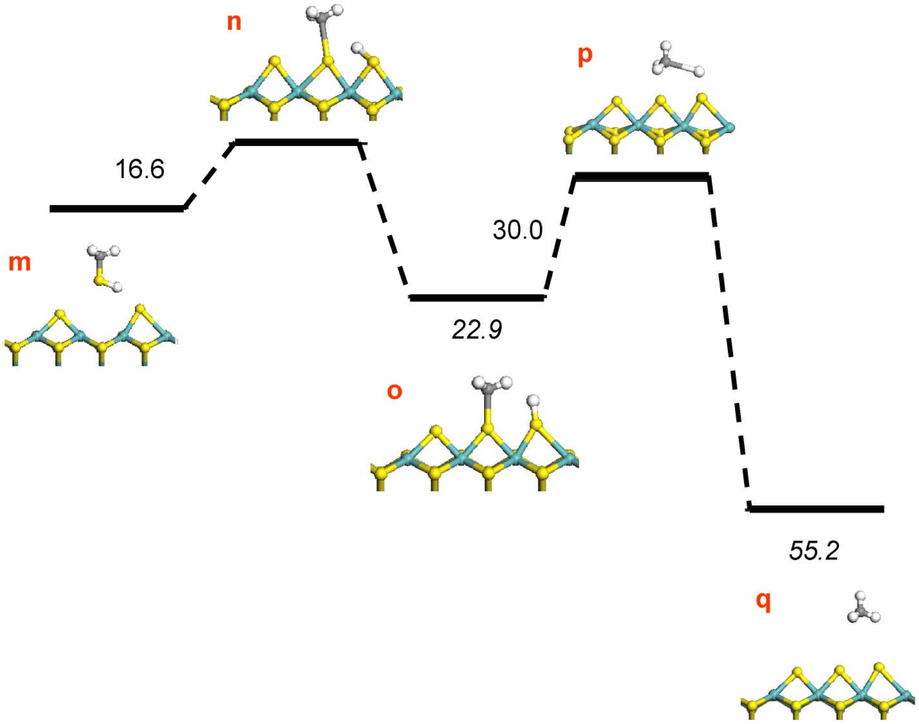

Fig. 5. Reaction path of the reaction of CH_3SH to CH_4 on the unpromoted Mo edge of 2H-MoS_2 with two sulfur atoms in bridging position.

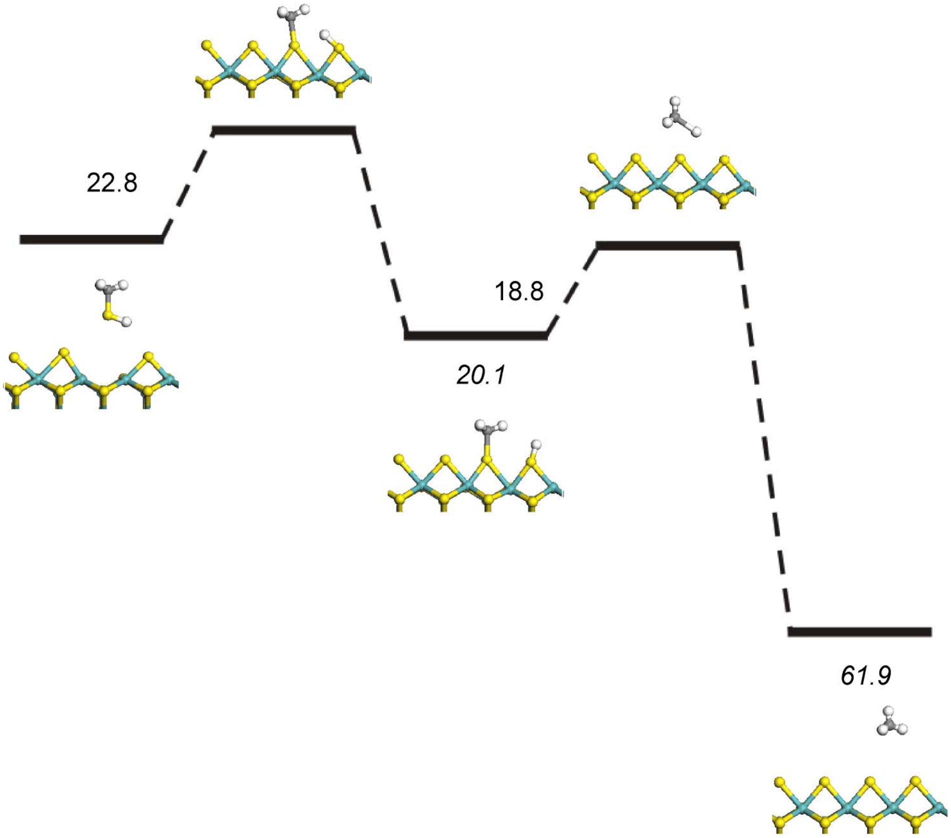

Fig. 6. Reaction path of the reaction of CH_3SH to CH_4 on the unpromoted Mo edge of 2H-MoS_2 with three sulfur atoms in bridging position.

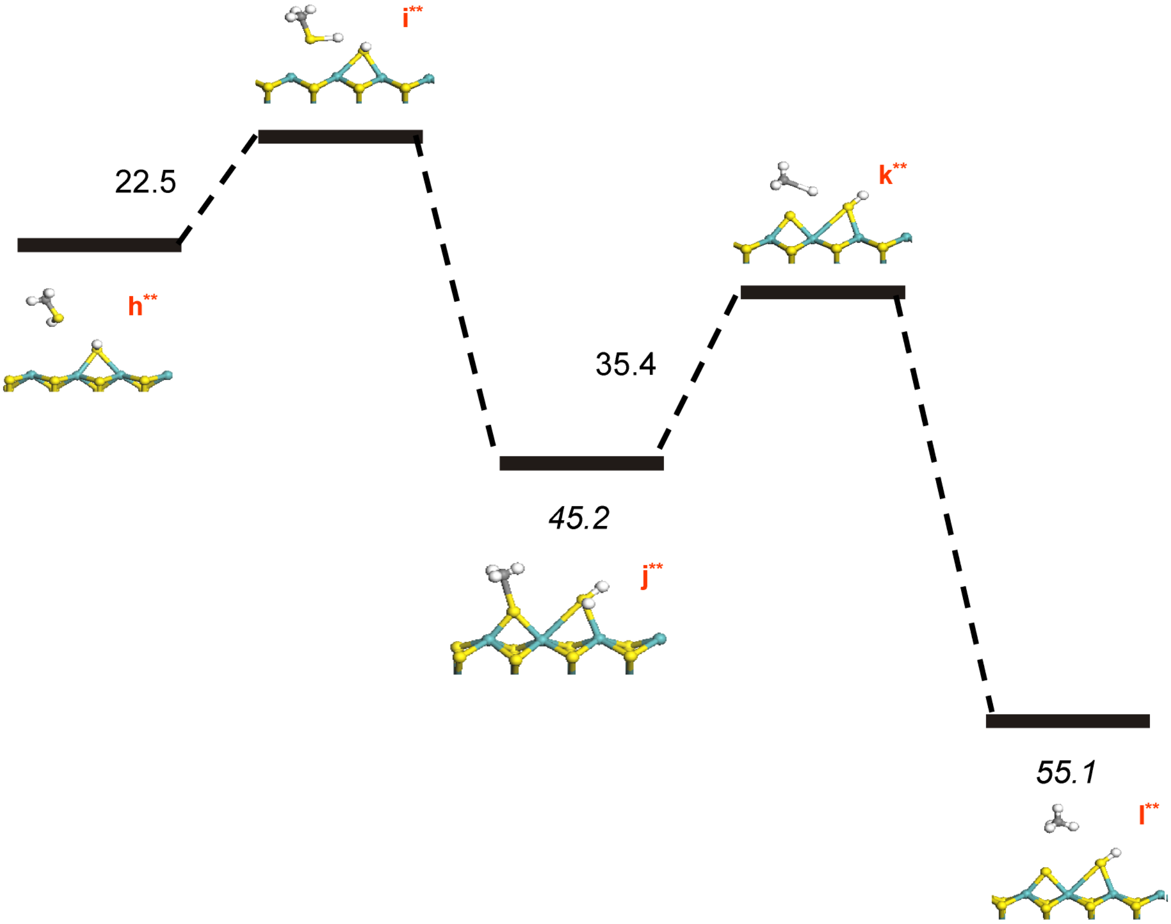

Fig. 7. Reaction path of the reaction of CH_3SH to CH_4 on the unpromoted Mo edge of 2H-MoS_2 with one SH group in bridging position.

Table 1
Activation energies and energy differences (in kcal/mol) in the reaction of CH_3SH to H_2S and CH_4 as a function of the number (N_{br}) of bridging S atoms on the Mo edge

Edge	N_{br}	$E_a(1)$	$-\Delta E(1)$	$E_a(2)$	$-\Delta E(2)$
Mo	0	12.6	46.4	68.6	19.9
	0	12.6	50.9	78.4	15.4
	1	18.8	38.9	46.0	29.6
	2	16.6	22.9	30.0	55.2
	3	22.8	20.1	18.8	61.9
	0 + SH	22.5	45.2	35.4	55.1
	2 + SH	26.8	44.7	34.6	58.4
Co–Mo	1	18.6	2.1	21.2	57.9
	2	21.2	2.0	19.1	58.2
Ni–Mo	1	19.4	5.1	19.3	58.9
	2	21.6	4.1	18.6	62.8

two S atoms and one SH group; the results are similar to those for the surface with an SH group only (Table 1).

3.1.2. *Co- and Ni-promoted Mo edge*

It is well known that the addition of Co or Ni significantly increases the catalytic activity of MoS_2-type catalysts [2]. For this reason, cobalt and nickel are referred to as promoter atoms. Although the origin of the promotional effect remains under study, the location of the promoter atoms has been clarified. Based on results of Mössbauer emission spectroscopy, Topsøe et al. proposed that the Co atoms are present on the Mo edges of the MoS_2 crystallites in Mo positions. These authors called the resulting structure the Co–Mo–S structure and used it to explain the promotional effect of cobalt on MoS_2 [50]. DFT calculations confirm that the promoter atoms are most likely located at the MoS_2 edges [51].

To study the effect of the promoter atoms on the CH_3SH dissociation process, we performed calculations similar to those for the unpromoted MoS_2 structure but with one surface Mo atom replaced by a promoter atom (Co or Ni). To remain consistent with our other calculations, we concentrated on structures with the promoter atoms on the metal edge. Note, however, that Co and Ni can also be present on the sulfur edge and that the structures with Co promoter atoms on the sulfur edge are slightly more stable than those with Co atoms on the metal edge [45,51]. Because the calculations on the Mo edge showed that the presence of sulfur atoms is beneficial for the hydrogenolysis of CH_3SH, we put at least one sulfur atom at the Co- or Ni-promoted surface in a bridging position between two Mo atoms. Furthermore, because DFT calculations have shown that incorporating promoter atoms leads to a reduced sulfur coverage of the metal edge [12,15,51], we considered only initial states with one or two sulfur atoms.

In the first calculations, we put one sulfur atom on the edge (Fig. 8). Geometric optimization of the initial, intermediate,

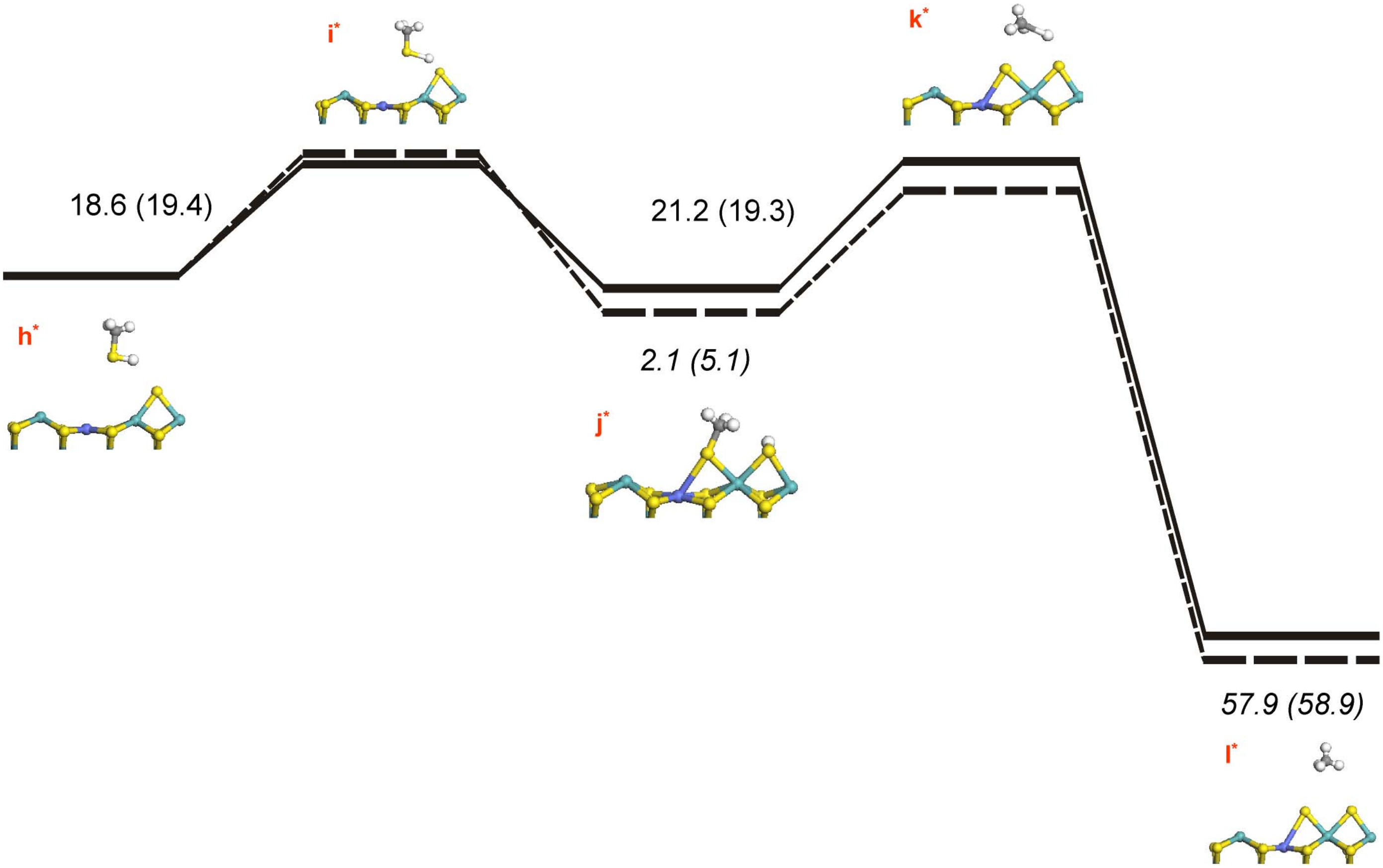

Fig. 8. Reaction path of the reaction of CH_3SH to CH_4 on the Co- and Ni-promoted Mo edge of 2H-MoS_2 with one sulfur atom in bridging position. The values for the Ni-promoted surface are given in parentheses.

and final structures relaxed the Co atom inward and shortened its distance to the neighbouring sulfur atoms to 2.25 Å. The cobalt atom and one of the molybdenum atoms on the surface were four-coordinated, whereas the other two Mo atoms were five-coordinated (h*). Because of the inward relaxation of the Co atom, the distance between the sulfur atom of the CH_3SH molecule and the surface Co atom increased from 4.5 Å for the unpromoted surface to 5 Å for the promoted surface, whereas the distance between the hydrogen atom of the CH_3SH molecule and the surface sulfur atom was 2.8 Å. Adsorption of CH_3SH on the surface had an energy barrier of 18.6 kcal/mol (h* → i*), almost the same as that for the unpromoted surface (Fig. 4). However, the CH_3S and H fragments were less strongly bound to the surface (i.e., favoured by only 2.1 kcal/mol (j*)), and thus the energy barrier of the subsequent step—breaking the C–S bond—decreased from 46.0 kcal/mol for the unpromoted surface to 21.2 kcal/mol. The final state, with two sulfur atoms in bridging positions on the surface (l*), was more stable than the intermediate state (j*) by 57.9 kcal/mol.

Similar calculations were performed with two sulfur atoms on the surface between the Mo atoms. In this situation the cobalt atom is four-coordinated, whereas two Mo atoms are five-coordinated and one Mo atom is six-coordinated. The results are similar to those when one sulfur atom is initially present on the surface (Table 1).

The Ni promoter also led to a less stable intermediate and a lower energy barrier for CH_4 desorption. The energy barrier for dissociation and adsorption of the CH_3S and H fragments to the surface was 19.4 kcal/mol (Fig. 8, h* → i*). The intermediate state (j*) was favoured by only 5.1 kcal/mol over the initial state (h*), whereas the final state (l*) was energetically preferred by 58.9 kcal/mol over the intermediate state. In the final state, CH_4 was formed and desorbed from the surface. The corresponding barrier for desorption was 19.3 kcal/mol, lower than for the unpromoted surface and slightly lower than for the Co-promoted surface. Similar calculations were performed with two sulfur atoms on the surface (Table 1).

3.2. Dissociation of CH_3SCH_3

In addition to the hydrogenolysis of methanethiol we studied the hydrogenolysis of dimethylsulfide (CH_3SCH_3) on a surface with one and two sulfur vacancies as the starting position. We calculated two different mechanisms. In the first one of the methyl groups of the adsorbed dimethylsulfide is transferred to a neighbouring adsorbed S atom, creating two CH_3S groups at the surface. This step had an activation energy of 15.8 kcal/mol and was exothermic by −24.1 kcal/mol. These CH_3S groups can form methane and adsorbed S atoms by reaction with adsorbed H atoms, as described above. The creation of these H

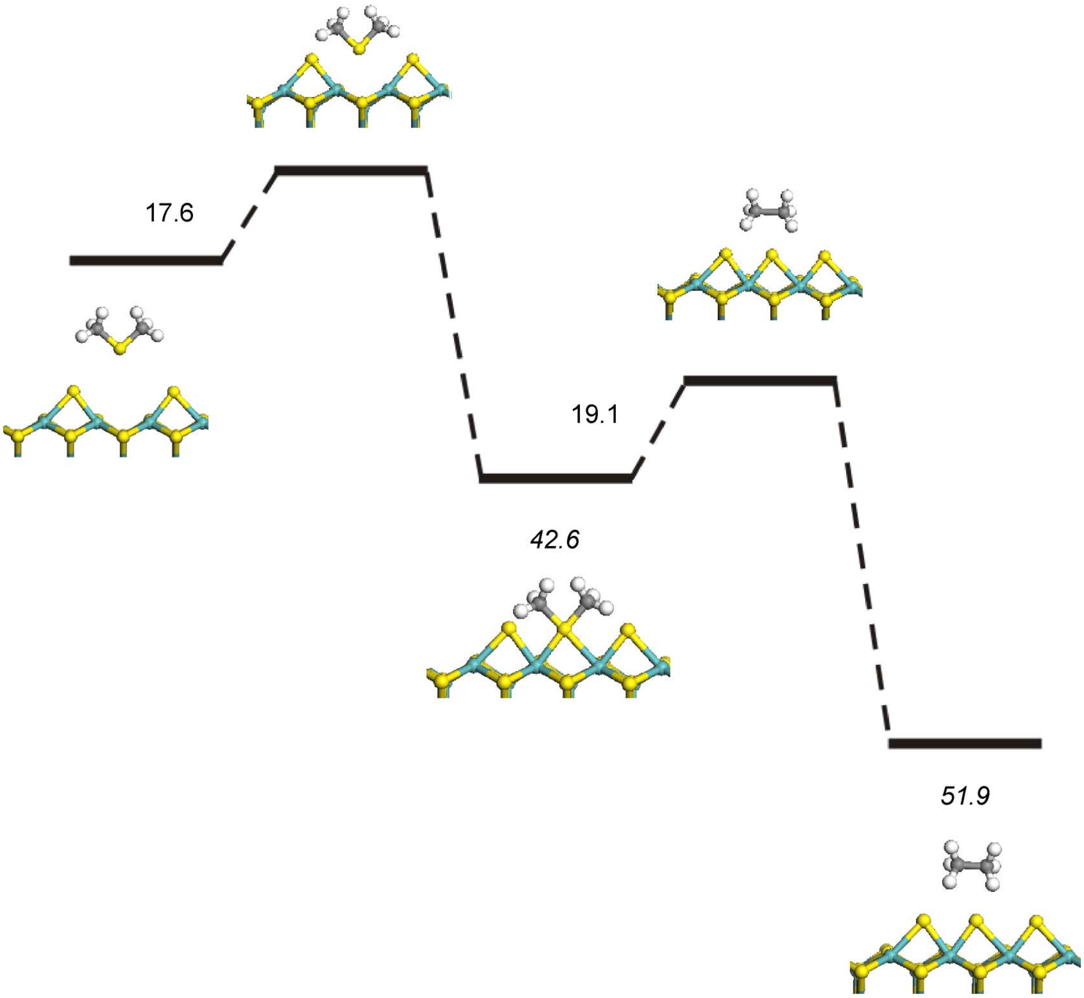

Fig. 9. Reaction path of the reaction of CH_3SCH_3 to C_2H_6 on the unpromoted Mo edge of 2H-MoS_2 with two sulfur atoms in bridging position.

Table 2
Activation energies and energy differences (in kcal/mol) in the reaction of CH_3SCH_3 to C_2H_6 as a function of the number (N_{br}) of bridging S atoms on the Mo edge

N_{br}	$E_a(1)$	$-\Delta E(1)$	$E_a(2)$	$-\Delta E(2)$
2	17.6	42.6	19.1	51.9
3	20.6	36.8	18.8	58.4

atoms by dissociative chemisorption of H_2 on the catalyst surface is discussed in the next section.

The other mechanism deals with the formation of ethane (which, however, is only a side product). The calculated reaction path for dimethylsulfide on the surface with two vacancies (Fig. 9) was similar to that of the hydrogenolysis of CH_3SH on the same surface (Fig. 5). Dimethylsulfide adsorbed with its S atom in the vacant position, bridging two Mo atoms. This adsorption had activation energy of 17.6 kcal/mol and was exothermic by 42.6 kcal/mol. The final step, combination of the methyl groups to ethane, had an activation energy of 19.1 kcal/mol and was exothermic by 51.9 kcal/mol. The results are very similar for the surface covered with one vacancy (Table 2).

3.3. *Hydrogen chemisorption and diffusion*

Understanding the role of hydrogen is of great importance in the study of desulfurization reactions. Although some results have already been published [8,9,15], we performed additional calculations on the adsorption and diffusion of the surface hydrogen to learn more about the dynamics on the catalytically active (100) MoS_2 edge structure. These additional calculations were needed for consistency reasons to obtain results for hydrogen dissociation and adsorption within the method and the parameters that we used. Our calculations show that the homolytic hydrogen dissociation and adsorption on the S edge is endothermic with a reaction energy of 43.5 kcal/mol and a barrier of 67.5 kcal/mol, whereas the heterolytic hydrogen adsorption on the bare Mo edge and the fully sulfided S edge is exothermic with a reaction energy of −3.3 kcal/mol and a barrier of 18.1 kcal/mol. This results in Mo–H and S–H surface fragments (Fig. 10a).

Starting with this situation and transferring the hydrogen from the Mo edge to the S edge, we found an energy barrier of 69.3 kcal/mol (Fig. 10, a → b). Thus, a reaction path passing through a local minimum on the potential energy surface

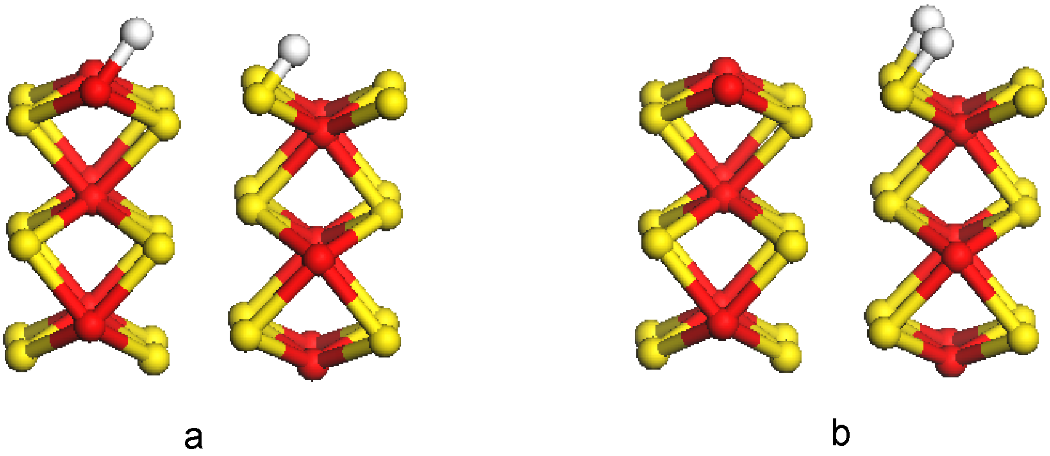

Fig. 10. Hydrogen transfer from the Mo to the S edge: (a) initial state, (b) final state.

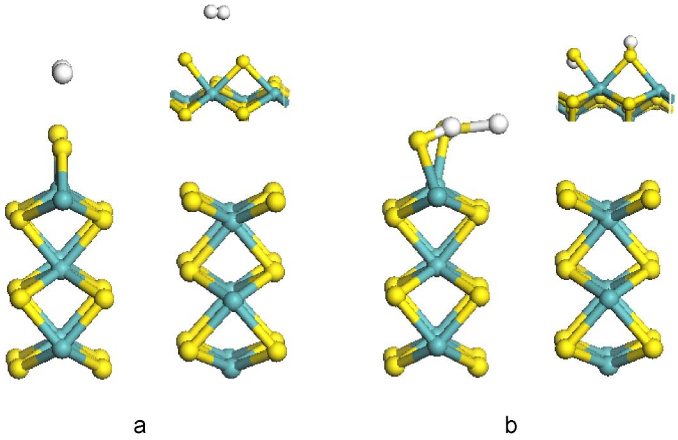

Fig. 11. Hydrogen adsorption on a sulfided Mo edge: (a) initial state, (b) final state.

on the Mo edge (with hydrogen split and adsorbed on the metal edge) is energetically demanding.

The adsorption of H_2 on the Mo edge fully covered with sulfur atoms in bridging positions, which is the most stable structure under hydrotreating conditions [13–15], was found to be endothermic, with a reaction energy of 32.1 kcal/mol and an energy barrier of 89 kcal/mol (Fig. 11). The strong endothermicity of the hydrogen dissociation on this surface might be due to the fact that the Mo atoms are fully coordinated and that there are no longer coordinatively unsaturated sites to bind the H atoms and thus compensate for the strong H–H bond. Dissociation of H_2 on the Mo edge covered by one sulfur atom led to one H atom bonded to the S atom bridging two Mo atoms and the other H atom bonded to one of these Mo atoms (Fig. 12). This reaction is endothermic (30.5 kcal/mol) and has an energy barrier of 33.5 kcal/mol. Transfer of the hydrogen atom from the Mo atom to the sulfur atom, giving adsorbed H_2S,

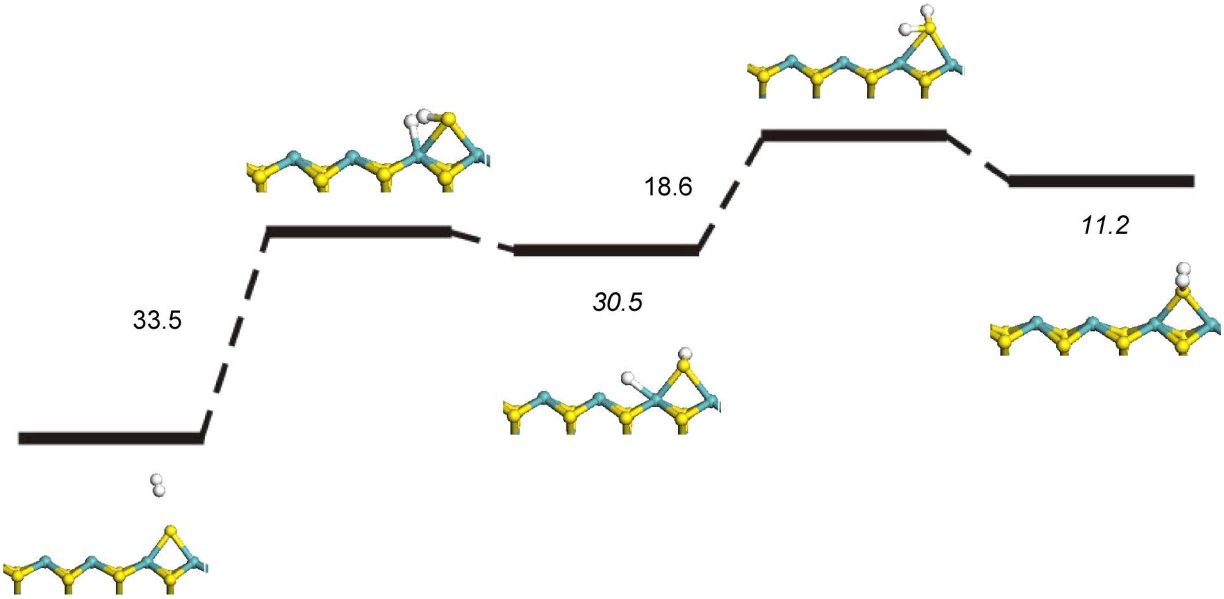

Fig. 12. Hydrogen dissociation, adsorption, and diffusion on the Mo edge with one bridging sulfur atom, resulting in the formation of adsorbed H_2S.

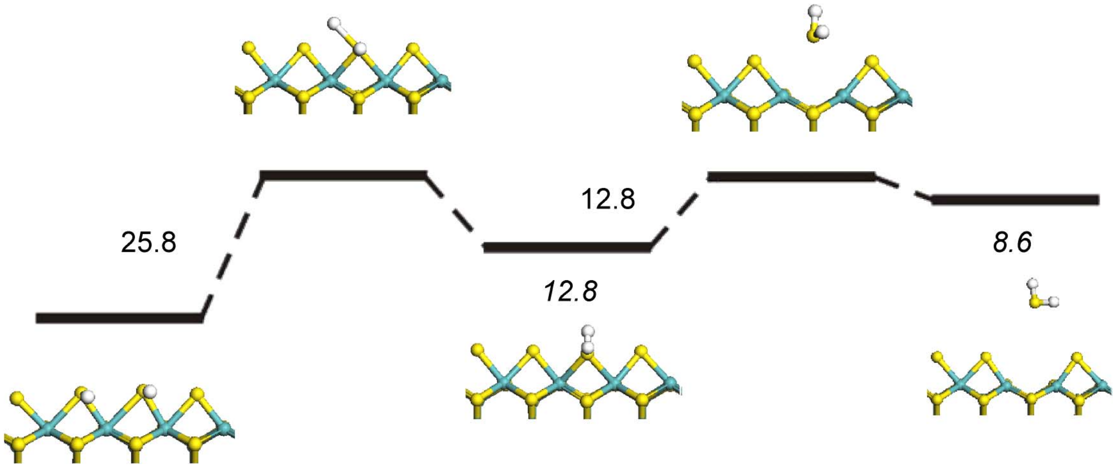

Fig. 13. Hydrogen diffusion along the sulfided Mo edge, resulting in the formation and removal of H_2S.

is endothermic by 11.2 kcal/mol and has an energy barrier of 18.6 kcal/mol. The calculated diffusion path of hydrogen in the present work differs slightly from that proposed by Paul and Payen, who also considered Mo–H species [52]. Mo–H surface species are likely to occur under certain conditions. A detailed investigation of their formation and properties will follow [53].

Hydrogen transfer along an edge is energetically less demanding than hydrogen transfer from the Mo edge to the S edge. Diffusion of a hydrogen atom on the sulfided Mo edge from one sulfur atom to the next (i.e., an exchange between a sulfur atom and an SH group) has an activation energy of only 5 kcal/mol, whereas diffusion of a hydrogen atom from a sulfur atom to an adjacent SH group has an energy barrier of 25.8 kcal/mol (the kinetic limiting step) and endothermic reaction energy of 12.8 kcal/mol (Fig. 13). As a result, adsorbed H_2S and a sulfur atom form from two SH groups. Removal of the resulting H_2S from the surface during the formation of a sulfur vacancy has an activation energy of 12.8 kcal/mol and an endothermic reaction energy of 8.6 kcal/mol. For a surface with one sulfur vacancy, these activation energies and energy differences were similar ($E_a(1) = 18.6$, $\Delta E(1) = 11.6$, $E_a(2) = 10.8$, and $\Delta E(2) = 10.2$ kcal/mol).

4. Discussion

4.1. Energy barrier dependence on the number of adsorbed sulfur atoms

The calculations show that the hydrogenolysis of methanethiol with dihydrogen to methane and H_2S occurs in several steps. First, methanethiol adsorbs and dissociates in a CH_3S fragment and an H atom. This reaction occurs between the initial state I (methanethiol, H_2, and the surface with n sulfur vacancies) and the intermediate state II (CH_3S, H_2, and the surface with $(n - 1)$ vacancies). In the second step, CH_3S reacts with an adsorbed H atom to methane, and the system moves from state II to state III (methane, H_2, and the surface with $(n - 1)$ vacancies). In the third step, the sulfur atom is removed from the surface by hydrogen atoms, which originate from the dissociative chemisorption of dihydrogen. The two-step reaction from state I to state III is strongly exothermic, and the energy of the intermediate state II relative to the energies of states I and III depends on the composition of the Mo edge. Adsorbed S and H atoms, as well as promoter atoms, influence the relative energies and thus the activation energies of the methanethiol dissociation and reaction to methane. This is clearly shown in the Brønsted–Evans–Polanyi relationship of the reaction II → III (Fig. 14b). However, there is no such clear relationship for the first part of the reaction (I → II, Fig. 14a). A possible explanation for this is that a sulfur coverage < 2 does not exist under real HDS conditions. Therefore, the energy values presented here are good reference points for a low sulfur coverage but cannot reveal the trends characteristic of actual working HDS conditions. This finding is in agreement with previous theoretical studies based on kinetic and thermodynamic considerations [11,12].

The calculated energy barriers for the dissociation of adsorbed CH_3SH to CH_3S and H and to CH_3 and SH fragments are low, whereas the energy barriers for the adsorption of the thiol on the surface, and especially for methane formation, are higher. For instance, dissociation of the adsorbed thiol on the bare surface is easy (4.5 kcal/mol) compared with thiol adsorption (12.6 kcal/mol) and the formation and removal of CH_4 from the surface (68.6 kcal/mol) (Fig. 2). The thermodynamic driving force for C–S bond scission in thiol desulfurization is the formation of a strong Mo–S bond [27]. The barrier $E_a(2)$ for the subsequent step, the reaction of CH_3 and hydrogen to CH_4, is reduced by the presence of S atoms on the metal edge (Table 1). As explained above, the barrier for the first step—thiol adsorption—increases at the same time. On the bare surface (Fig. 2), association of the thiol is a relatively easy step with an energy barrier of 12.6 kcal/mol, but formation of CH_4 from adsorbed CH_3 and SH has a high barrier (68.6 kcal/mol). A preadsorbed sulfur atom makes adsorption more difficult (18.8 kcal/mol) but substantially reduces the energy barrier for CH_4 formation, to 46.0 kcal/mol (Fig. 4). Adding a second S atom to the surface further reduces the energy barrier to 30.0 kcal/mol (Fig. 5) to form CH_4, and a third S atom reduces it even further, to 18.8 kcal/mol. The adsorption and reaction of CH_3SH on the catalytically active (100) surface of MoS_2 thus

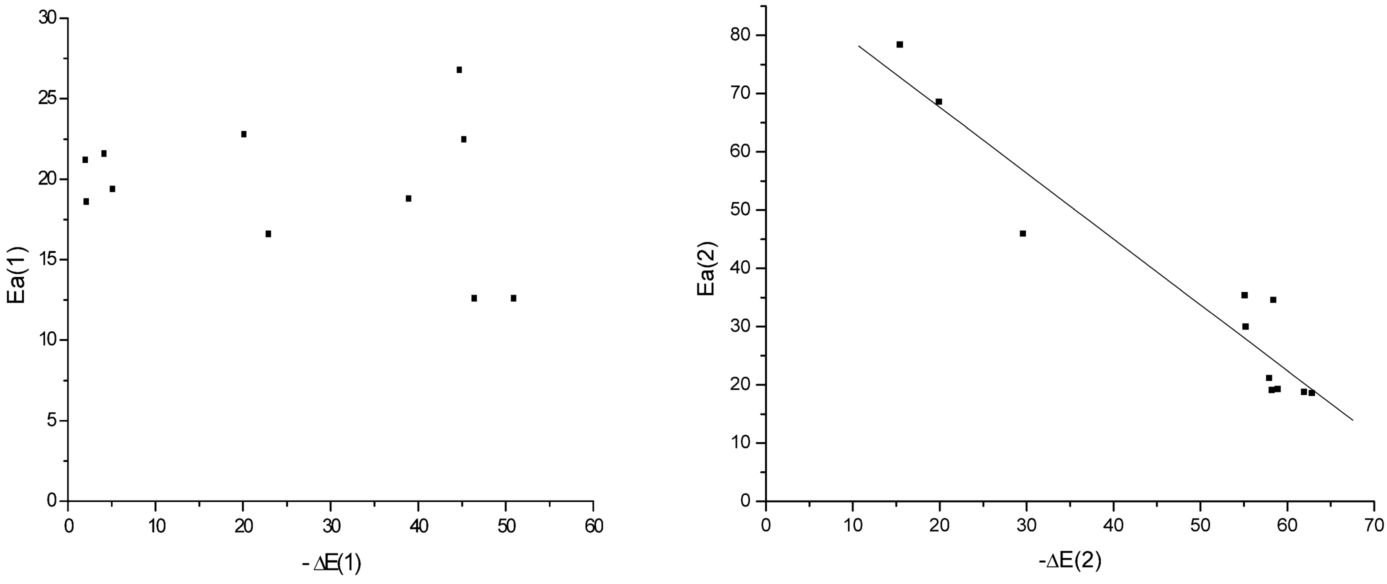

a

b

Fig. 14. Activation energies as a function of energy differences: (a) initial – intermediate state, (b) intermediate – final state.

clearly depend on the number of adsorbed sulfur atoms and on the nature of the exposed active surface sites.

The energy of the intermediate state of adsorbed CH_3S depends on the sulfur coverage of the Mo edge of MoS_2. The adsorption energy of CH_3SH (dissociating to CH_3S and H fragments) decreases with increasing S coverage of the Mo edge from 50.9 to 20.1 kcal/mol (Table 1). Similarly, the adsorption energy of atomic sulfur on transition-metal surfaces varies between 80 and 140 kcal/mol and decreases substantially with increasing S coverage [54]. This decrease can be explained by the effective medium theory [55]. According to this theory, the adsorption energy of an adsorbate depends on the energy gain from embedding the atoms of the adsorbate in the surface electron gas and on the energy loss from incomplete screening of the electrostatic interaction between the adsorbate and the surface ionic nuclei. The higher the metal coordination number, the broader the d band and hence the lower the energy of the d band centre. Adsorption on the Mo edge increases the metal coordination number and thus lowers the energy of the d band and the interaction with adsorbate molecules.

4.2. *Comparison with pure metal surfaces*

Dissociation of organosulfur molecules is much more difficult on MoS_2 than on metal surfaces. When MoS_2 is exposed to organosulfur molecules, hydrocarbons and H_2S form and desorb to the gas phase. But on metals, not only do H_2 and hydrocarbon species desorb to the gas phase, but also S and C atoms remain on the surface. Clean W(211) [29], Ni(110) [32], Ni(100) [33], and Ni(111) [34] surfaces break many molecules completely to adsorbed atomic fragments at low coverage. Adsorbed oxygen, sulfur, and carbon atoms weaken the strong reducing power of the metallic surfaces and lead to adsorbed molecular fragments. The exact surface chemistry of organosulfur molecules depends on the metal and the complexity of the organosulfur molecule. In general, the S–H bond in H_2S and thiols breaks below 200 K, whereas the S–C bond in thiols and thiophene cleaves between 250 and 400 K [27,34]. These temperatures are much lower than the temperatures required for bond breakage over MoS_2. This demonstrates that the sulfur atoms below the surface Mo atoms on the Mo edge of MoS_2 weaken the ability of the Mo atoms for cleaving bonds, just as O, S, and C atoms do on the metal surface, to such an extent that C–C bonds cannot be broken, and thus no valuable fuel molecules are lost. However, bond breakage is sufficient to break C–S bonds, and hence to remove sulfur atoms from organosulfur molecules in fuels.

4.3. *Role of the promoters*

The decrease of the sulfur–metal bond energy as a function of the sulfur coverage revealed in the present work is consistent with results from previous theoretical investigations of transition metal sulfide systems. Our investigation of the hydrogenolysis reaction of CH_3SH to CH_4 on the same systems was based on the findings of Raybaud et al. [11,12] that the nature and the concentration of the active sites vary in the reactive atmosphere above the surface. Furthermore, the incorporation of promoter atoms has an influence on the sulfur–metal bond energy at the surface, leading in particular to a reduced equilibrium sulfur coverage of the active metal sites.

Not only sulfur atoms, but also Co and Ni promoter atoms, lead to a less strongly bound CH_3S intermediate and thus to a lower barrier for CH_4 formation and desorption from the surface. Activation energies of 19.1 and 18.6 kcal/mol were obtained for CH_4 formation over the Co–Mo and Ni–Mo edges with two bridging S atoms, respectively, whereas 18.8 kcal/mol was the lowest activation energy obtained for the unpromoted

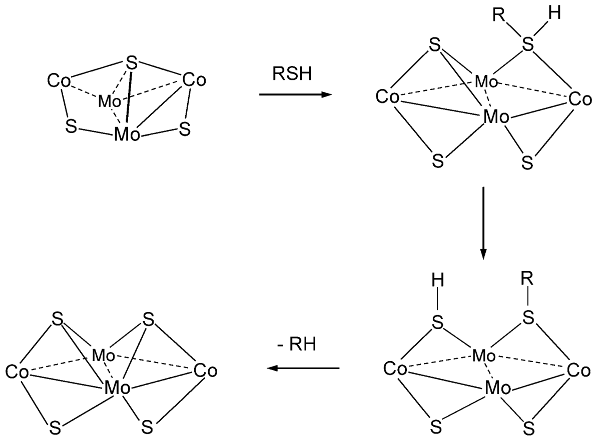

Scheme 1. Adsorption of an alkane- or arenethiol on the $Cp'_2Mo_2Co_2S_3(CO)_4$ cluster (Cp' = pentamethylcyclopentadienyl), followed by activation and cleavage of the C–S bond, and formation of a hydrocarbon (Mo = MoCp′, Co = $Co(CO)_2$).

Mo edge (Table 1). A parallel can be drawn between this low activation energy for C–S bond breaking on the Co–Mo edge and the conclusion drawn by Curtis and coworkers [35,36] that the association of the aliphatic thiols with a $Cp'_2Mo_2Co_2S_3(CO)_4$ cluster is the rate-determining step in the reaction of the thiols. The bridge bonding of the RS group between metal atoms of the $Cp'_2Mo_2Co_2S_3(CO)_4$ cluster led to the activation of the C–S bond and eased the subsequent cleavage of the C–S bond (Scheme 1). In general, the activation energy $E_a(2)$ for the S–C bond breaking is not significantly modified by the promoter atom. This implies that the role of the promoter atom is not to facilitate the S–C bond breaking, but rather to lower the barrier for product desorption from the surface. Another possible explanation might be that the promoter is not activated when incorporated on the metal edge of the catalyst.

4.4. *Regeneration of the active site*

After the adsorption and reaction of CH_3SH to methane and a sulfur atom adsorbed on the catalyst surface, the sulfur atom must be removed, so that the catalytic cycle of the reaction of methanethiol and H_2 to methane and H_2S is closed. The removal of sulfur and creation of a vacancy for subsequent adsorption of CH_3SH is achieved by dihydrogen. H_2 splits on the sulfided Mo-terminated edge and forms two SH groups with an energy barrier of 89 kcal/mol and an endothermic reaction energy of 32.1 kcal/mol. Cristol et al. [13,14] and Travert et al. [15] also found that the dissociation of H_2 on the fully covered Mo edge is endothermic, although less strong than in our case, whereas Sun et al. calculated H_2 adsorption to be slightly exothermic [47]. For Co–Mo–S surfaces, in contrast, the H_2 dissociation was calculated to be exothermic and not strongly activated [15].

Diffusion of hydrogen over the fully sulfided Mo edge and formation of molecularly adsorbed H_2S costs 12.8 kcal/mol (Fig. 13). Desorption of H_2S from the surface leaves a surface with a sulfur vacancy and H_2S in the gas phase and is endothermic by 8.6 kcal/mol. Thus the second step of the regeneration of the catalyst surface—creation of the coordinatively unsaturated site on the Mo edge—is endothermic by 21.4 kcal/mol (Fig. 13). Therefore, the whole process of regeneration of the active site and closing of the catalytic cycle (i.e., H_2 dissociation, H diffusion on the sulfided surface, H_2S formation, and desorption) is endothermic by 53.5 kcal/mol. If only one S atom is left on the Mo-terminated edge, then the process of regeneration of the active site occurs by first dissociating H_2 on the Mo and S atoms. This endothermic reaction costs 30.5 kcal/mol. Then H_2S forms by diffusion of the H atom from the Mo atom to the S atom (endothermic by 11.2 kcal/mol), and finally H_2S is desorbed (endothermic by 10.8 kcal/mol). The overall regeneration process of the active site thus costs 52.5 kcal/mol. With these regenerations of the active sites, energies of -14.4 and -13.8 kcal/mol are calculated for the overall hydrogenolysis reaction of $CH_3SH + H_2 \rightarrow CH_4 + H_2S$ on the surface with one S vacancy (Fig. 5) and the surface with three S vacancies (Fig. 3), respectively. These values are in good agreement with the experimental value of -17 kcal/mol and lend support to the theoretical approach that we used.

Comparing Figs. 5 and 6 shows that the energy of the final state after dissociation of methanethiol and the formation of methane and an adsorbed sulfur atom is not as low for the promoted surface as for the Mo-only surface. This is a result of the weaker Co–S and Ni–S bonds compared with the Mo–S bond. Consequently, the energy required to remove the sulfur atom from the surface by hydrogenation to H_2S is 18 (Co–Mo surface) or 14 kcal/mol (Ni–Mo surface) lower than for the Mo surface. This indicates that the promoter also decreases the adsorption energy of the sulfur atom from methanethiol on the catalyst surface and thus decreases the sulfur-removing energy.

The calculated activation energies can be compared with the experimental activation energies of 22.9 and 22.0 kcal/mol for the hydrogenolysis of methanethiol and dimethylsulfide to methane and H_2S over unsupported MoS_2, respectively, and 19.7 kcal mol for the formation of dimethylsulfide from methanethiol [26]. In the case of zero-order conditions, the experimental activation energy is equal to the activation energy of the rate-determining step; in the case of first-order conditions, it should be equal to the activation energy of that step minus the heat of adsorption of the reactants. Because the hydrogenolysis of methanethiol was studied under zero-order conditions, the observed activation energy should be compared with the largest activation energy of the different reaction steps. In our case this is clearly H_2 dissociation followed by sulfur atom removal. In addition, DFT calculation of the HDS of thiophene on the bare Mo edge of (100) MoS_2 indicated that sulfur removal is the rate-determining step and that its energy cost depends on the sulfur coverage of the Mo edge [11]. In contrast, on a metallic Ni(111) surface, C–S bond breaking was suggested to be the rate-determining step for methane formation from methanethiol [34], whereas a DFT calculation for small nickel sulfide clusters found S–C bond scission and sulfur removal to be about equally slow and rate-determining for thiophene desulfurization [56]. A possible explanation for this difference is that the Ni–S bond is weaker than the Mo–S bond, and thus stabilization of the sulfur-containing intermediates is lower on nickel sulfide. The strong binding of CH_3S on the Mo edge of (100) MoS_2 is a consequence of Mo–S interactions involving the occupied sulfur lone pairs of the molecule and the empty 4d orbitals of molybdenum.

4.5. *An overview of the investigated mechanisms*

The calculations demonstrate that the hydrogenolysis reaction of methanethiol is not a concerted reaction of C–S bond breaking and C–H and S–H bond creation, but rather occurs in two steps. In the first step, the S–H bond of methanethiol is broken and a CH_3S group is adsorbed on the surface. This adsorbed CH_3S and a neighbouring adsorbed SH group react to methane and two surface sulfur atoms. In the second step, one of the sulfur atoms is removed from the surface by reaction with two adsorbed hydrogen atoms to H_2S desorbing from the surface. The chemistry that occurs is radical chemistry, as it were. The metal sulfide surface stabilizes the CH_3S, H, and SH radicals and allows them to react with each other. But the chemistry is not the same as on the surface of a metal, where alkanethiols decompose to alkyl groups and sulfur and hydrogen atoms that all become attached to metal atoms. Instead, on the metal sulfide surface, the alkyl and hydrogen fragments are bonded to sulfur atoms, and they react with one another on these sulfur atoms other to alkanes. The results from this study show that in the presence of adsorbed sulfur atoms, methanethiol and dimethylsulfide react as follows:

$$\text{X–S–Y} + * + \text{S}* \rightarrow \text{X–S}* + \text{Y–S}* \rightarrow \text{X–Y} + 2\text{S}*, \qquad (1)$$

where X, Y = CH_3 or H, and * indicates a site consisting of one or two Mo atoms.

Thus,

$$H_2S + * + S* \rightarrow 2\text{H–S}* \rightarrow H_2 + 2S*$$

and

$$CH_3SH + * + S* \rightarrow CH_3\text{–S}* + \text{H–S}* \rightarrow CH_4 + 2S*.$$

On the bare Mo edge, methanethiol adsorption and decomposition occur slightly differently,

$$CH_3SH + 2* \rightarrow CH_3* + HS* \rightarrow CH_4 + S* + *. \qquad (2)$$

Because in reality the Mo edge is (almost) fully covered with S atoms, reactions (2) are not important for catalysis. Reaction (1) predicts that ethane may be formed from dimethylsulfide (X = Y = CH_3), and the calculations show that this reaction has a similar activation barrier as the reaction of methanethiol (X = CH_3 and Y = H) to CH_4. Nevertheless, experimentally, ethane has not been observed in the HDS of dimethylsulfide. The reason for this is probably that the reaction of dimethylsulfide to two CH_3S groups is faster than the reaction to ethane, as suggested by the lower activation energy for the reaction of dimethylsulfide to two CH_3S groups.

The same chemistry responsible for the reaction of alkanethiols to alkanes may be responsible for the reaction of dibenzothiophene to biphenyl. Dibenzothiophene is exemplary for molecules present in gas oil, and its sulfur atom is removed mainly by direct desulfurization, an apparent hydrogenolysis reaction. Surface science studies of the reaction of the related benzenethiol on metal surfaces have indeed shown a great similarity with the reactions of alkanethiols [57–60]. The S–H bond of benzenethiol is already broken at low temperature, and the resulting C_6H_5S reacts to benzene below room temperature. This suggests that the hydrodesulfurization of arylthiols, such as benzenethiol, benzothiophene, and dibenzothiophene, on metal sulfides occurs in the same way as the hydrogenolysis of alkanethiols and dialkylsulfides.

4.6. *Implications for hydrotreating catalysis*

It has been shown that the dissociation of CH_3SH on different edge surfaces of MoS_2 occurs on a pair of sulfur–metal sites to form an S–H group and CH_3S species that are adsorbed in bridging positions between two metal surface atoms, followed by transfer of hydrogen to the neighbouring CH_3S species to form CH_4. The mechanism is similar to that proposed for the dissociation of H_2 [47,52] and reveals a similar behaviour for small molecules when dissociated and adsorbed on catalyst surfaces. However, the difference in the geometric structures and chemical properties of these sulfur–metal pairs is clearly affected by the amount of sulfur present on the metal edge surface. Therefore, different energy barriers for adsorption and desorption have been calculated, determining a different kinetic behaviour. Low sulfur coverage on the metal surface is not likely to exist under real HDS conditions, as confirmed in Fig. 14, despite the lower energy barriers for dissociation when the metal atoms are uncovered. But metal edges completely covered by sulfur will contribute to associative, rather than dissociative, mechanisms. Furthermore, to achieve a concerted reaction with moderate energy barriers for adsorption and desorption, our calculations favour about 67% coverage of the molybdenum edge by sulfur atoms.

5. Conclusion

The present calculations demonstrate that the hydrogenolysis reaction of methanethiol is not a concerted reaction, but rather occurs in consecutive steps. First, the S–H bond is broken and a CH_3S group is formed on the surface, which then reacts with a neighbouring adsorbed SH group to methane. Finally, a sulfur atom is removed from the surface by reacting with adsorbed hydrogen atoms to H_2S. Sulfur, promoter, and hydrogen atoms strongly affect the adsorption and reaction of methanethiol on the MoS_2 catalyst surface. At low sulfur coverage of the surface, the thiol adsorption has low activation energy, but the subsequent cleavage of the C–S bond and formation of methane is difficult. The C–S bond in adsorbed CH_3S is broken by reaction with the H atom on a neighbouring S atom, leaving the S atom on the surface and freeing CH_4 to the gas phase. Sulfur atoms adsorbed on the catalyst surface lower the activation energy for the reaction of CH_3S to methane. In addition, hydrogen atoms adsorbed on sulfur atoms at the catalyst surface and promoter atoms (Co and Ni) direct the hydrogenolysis to less strongly bound CH_3S and lower the energy barrier for CH_4 desorption from the surface in the dissociation of CH_3SH.

Although the reactions of methanethiol on metal sulfide surfaces have many similarities with reactions on metal surfaces, the chemistry is not the same. On the metal sulfide surface, the alkyl and hydrogen fragments are bonded to sulfur atoms, not to metal atoms. The results presented here also suggest that the hydrogenolysis of benzenethiol and dibenzothiophene occur by a similar mechanism.

Acknowledgments

We thank Prof. Dr. J.A.R. van Veen for valuable discussions. This work was supported by Shell Global Solutions International BV.

References

[1] R. Prins, V.H.J. de Beer, G.A. Somorjai, Catal. Rev.-Sci. Eng. 31 (1989) 1.
[2] H. Topsøe, B.S. Clausen, F.E. Massoth, Hydrotreating Catalysis, Science and Technology, Springer, Berlin, 1996.
[3] M.J. Girgis, B.C. Gates, Ind. Eng. Chem. Res. 30 (1991) 2021.
[4] D.D. Whitehurst, T. Isoda, I. Mochida, Adv. Catal. 42 (1998) 345.
[5] M. Egorova, R. Prins, J. Catal. 225 (2004) 417.
[6] M.C. Zonnevylle, R. Hoffmann, Surf. Sci. 199 (1988) 320.
[7] P. Raybaud, J. Hafner, G. Kresse, H. Toulhoat, Phys. Rev. Lett. 80 (1998) 1481.
[8] S. Cristol, J.F. Paul, E.F. Payen, D. Bougeard, F. Hutschka, J. Hafner, Stud. Surf. Sci. Catal. 128 (1999) 327.
[9] L.S. Byskov, J.K. Nørskov, B.S. Clausen, H. Topsøe, J. Catal. 187 (1999) 109.
[10] L.S. Byskov, J.K. Nørskov, B.S. Clausen, H. Topsøe, Catal. Lett. 64 (2000) 95.
[11] P. Raybaud, J. Hafner, G. Kresse, S. Kasztelan, H. Toulhoat, J. Catal. 189 (2000) 129.
[12] P. Raybaud, J. Hafner, G. Kresse, S. Kasztelan, H. Toulhoat, J. Catal. 190 (2000) 128.
[13] S. Cristol, J.F. Paul, E. Payen, D. Bougeard, S. Clemendot, F. Hutschka, J. Phys. Chem. B 104 (2000) 11220.
[14] S. Cristol, J.F. Paul, E. Payen, D. Bougeard, S. Clemendot, F. Hutschka, J. Phys. Chem. B 106 (2002) 5659.
[15] A. Travert, H. Nakamura, R.A. van Santen, S. Cristol, J.F. Paul, E. Payen, J. Am. Chem. Soc. 124 (2002) 7084.
[16] S. Cristol, J.F. Paul, E. Payen, D. Bougeard, F. Hutschka, S. Clemendot, J. Catal. 224 (2004) 138.
[17] T. Todorova, V. Alexiev, R. Prins, Th. Weber, Phys. Chem. Chem. Phys. 6 (2004) 3023.
[18] G.H. Spies, R.J. Angelici, Organometallics 6 (1987) 1897.
[19] R.J. Angelici, Coord. Chem. Rev. 105 (1990) 61.
[20] R.J. Angelici, in: Th. Weber, R. Prins, R.A. van Santen (Eds.), Transition Metal Sulphides, Chemistry and Catalysis, Kluwer Academic, Dordrecht, 1998, p. 89.
[21] W.D. Jones, L. Dong, J. Am. Chem. Soc. 113 (1991) 559.
[22] W.D. Jones, D.A. Vicic, R.M. Chin, J.H. Roache, A.W. Myers, Polyhedron 16 (1997) 3115.
[23] C. Bianchini, A. Meli, M. Peruzzini, F. Vizza, P. Frediani, V. Herrera, R.A. Sanchez-Delgado, J. Am. Chem. Soc. 115 (1993) 2731.
[24] C. Bianchini, A. Meli, in: Th. Weber, R. Prins, R.A. van Santen (Eds.), Transition Metal Sulphides, Chemistry and Catalysis, Kluwer Academic, Dordrecht, 1998, p. 129.
[25] F. Bataile, J.L. Lemberton, P. Michaud, G. Pérot, M. Vrinat, M. Lemaire, E. Schulz, M. Breysse, S. Kasztelan, J. Catal. 191 (2000) 409.
[26] R.L. Wilson, C. Kemball, J. Catal. 3 (1964) 426.
[27] B.C. Wiegand, C.M. Friend, Chem. Rev. 92 (1992) 491.
[28] R.J. Koestner, J. Stöhr, J.L. Gland, E.B. Kollin, F. Sette, Chem. Phys. Lett. 120 (1985) 285.
[29] J.B. Benziger, R.E. Preston, J. Phys. Chem. 89 (1985) 5002.
[30] J.T. Roberts, C.M. Friend, J. Am. Chem. Soc. 108 (1986) 7204.
[31] C.M. Friend, J.T. Roberts, Acc. Chem. Res. 21 (1988) 394.
[32] D.R. Huntley, J. Phys. Chem. 93 (1989) 6156.
[33] M.E. Castro, S. Ahkter, A. Golchet, J.M. White, T. Sahin, Langmuir 7 (1991) 126.
[34] T.S. Rufael, D.R. Huntley, D.R. Mullins, J.L. Gland, J. Phys. Chem. B 99 (1995) 11472.
[35] U. Riaz, O.J. Curnow, M.D. Curtis, J. Am. Chem. Soc. 116 (1994) 4357.
[36] M.D. Curtis, S.H. Druker, J. Am. Chem. Soc. 119 (1997) 1027.
[37] B. Delley, J. Chem. Phys. 92 (1990) 508.
[38] B. Delley, J. Chem. Phys. 113 (2000) 7756.
[39] S.H. Vosko, L. Wilk, M. Nusair, Can. J. Phys. 58 (1980) 1200.
[40] J.P. Perdew, Y. Wang, Phys. Rev. B 45 (1992) 13244.
[41] J.P. Perdew, J.A. Chevary, S.H. Vosko, K.A. Jackson, M.R. Peterson, D.J. Singh, C. Fiolhais, Phys. Rev. B 46 (1992) 6671.
[42] N. Govind, M. Petersen, G. Fitzgerald, D. King-Smith, J. Andzelm, Comput. Mat. Sci. 28 (2003) 250.
[43] T.A. Halgren, W.N. Lipscomb, Chem. Phys. Lett. 49 (1977) 225.
[44] S. Helveg, J.V. Lauritsen, E. Lægsgaard, I. Stensgaard, J.K. Nørskov, B.S. Clausen, H. Topsøe, F. Besenbacher, Phys. Rev. Lett. 84 (2000) 951.
[45] J.V. Lauritsen, S. Helveg, E. Lægsgaard, I. Stensgaard, B.S. Clausen, H. Topsøe, F. Besenbacher, J. Catal. 197 (2001) 1.
[46] J.V. Lauritsen, M.V. Bollinger, E. Lægsgaard, K.W. Jacobsen, J.K. Nørskov, B.S. Clausen, H. Topsøe, F. Besenbacher, J. Catal. 221 (2004) 510.
[47] M. Sun, A.E. Nelson, J. Adjaye, Catal. Today 105 (2005) 36.
[48] B. Hammer, J.K. Nørskov, Adv. Catal. 45 (2000) 71.
[49] C.M. Friend, J.T. Roberts, Acc. Chem. Res. 21 (1998) 394.
[50] H. Topsøe, B.S. Clausen, R. Candia, C. Wivel, S. Mørup, J. Catal. 68 (1984) 433.
[51] H. Schweiger, P. Raybaud, G. Kresse, H. Toulhoat, J. Catal. 212 (2002) 33.
[52] J.F. Paul, E. Payen, J. Phys. Chem. 107 (2003) 4057.
[53] T. Todorova, V. Alexiev, R. Prins, Th. Weber, in preparation.
[54] J.A. Rodriguez, J. Hrbek, Acc. Chem. Res. 32 (1999) 719.
[55] K.W. Jacobsen, J.K. Nørskov, M. Puska, J. Phys. Rev. B 35 (1987) 7423.
[56] M. Neurock, R.A. van Santen, J. Am. Chem. Soc. 116 (1994) 4427.
[57] C.W.J. Bol, C.M. Friend, H. Xu, Langmuir 12 (1996) 6083.
[58] D.A. Chen, C.M. Friend, H. Xu, Surf. Sci. 395 (1998) L221.
[59] S.M. Kane, T.S. Rufael, J.L. Gland, D.R. Huntley, D.A. Fischer, J. Phys. Chem. 101 (1997) 8486.
[60] S.M. Kane, D.R. Huntley, J.L. Gland, J. Phys. Chem. 102 (1998) 10216.